


Tyrosine phosphorylation of the lectin receptor-like kinase LORE regulates plant immunity

Xuming Luo^{1,2,†}, Wei Wu^{1,3,†}, Yingbo Liang^{1,2,†}, Ning Xu¹, Zongyi Wang⁴, Huasong Zou³ & Jun Liu^{1,2,*} 

Abstract

Plant pattern recognition receptors (PRRs) perceive pathogen-associated molecular patterns (PAMPs) to activate immune responses. Medium-chain 3-hydroxy fatty acids (mc-3-OH-FAs), which are widely present in Gram-negative bacteria, were recently shown to be novel PAMPs in *Arabidopsis thaliana*. The *Arabidopsis* PRR LIPOOLIGOSACCHARIDE-SPECIFIC REDUCED ELICITATION (LORE) is a G-type lectin receptor-like kinase that recognizes mc-3-OH-FAs and subsequently mounts an immune response; however, the mechanisms underlying LORE activation and downstream signaling are unexplored. Here, we report that one of the mc-3-OH-FAs, 3-OH-C10:0, induces phosphorylation of LORE at tyrosine residue 600 (Y600). Phosphorylated LORE subsequently trans-phosphorylates the receptor-like cytoplasmic kinase PBL34 and its close paralogs, PBL35 and PBL36, and therefore activates plant immunity. Phosphorylation of LORE Y600 is required for downstream phosphorylation of PBL34, PBL35, and PBL36. However, the *Pseudomonas syringae* effector HopAO1 targets LORE, dephosphorylating the tyrosine-phosphorylated Y600 and therefore suppressing the immune response. These observations uncover the mechanism by which LORE mediates signaling in response to 3-OH-C10:0 in *Arabidopsis*.

Keywords 3-OH-C10:0; innate immunity; LORE; receptor-like cytoplasmic kinase; tyrosine phosphorylation

Subject Categories Microbiology, Virology & Host Pathogen Interaction; Plant Biology; Signal Transduction

DOI 10.15252/embj.2019102856 | Received 3 July 2019 | Revised 7 December 2019 | Accepted 16 December 2019 | Published online 10 January 2020

The EMBO Journal (2020) 39: e102856

Introduction

Plants are constantly exposed to potential phytopathogens and have evolved an efficient innate immune system that protects them from infection. Cell surface-localized pattern recognition receptors (PRRs) and cytoplasmic immune receptors are classic plant immune receptors that perceive pathogen-associated molecular patterns (PAMPs)

and pathogen-secreted effectors, respectively (Couto & Zipfel, 2016). PAMPs are the essential, slow-evolving molecular signatures of microbes, such as the bacterial molecules flagellin, elongation factor Tu (EF-Tu), and lipopolysaccharide (LPS), and the fungal molecule chitin (Couto & Zipfel, 2016; Zipfel & Oldroyd, 2017). Following pathogen invasion, PRRs perceive PAMPs and activate immune responses, including a reactive oxygen species (ROS) burst, Ca²⁺ influx, mitogen-activated protein kinase (MAPK) activation, salicylic acid accumulation, and callose deposition, in a process referred to as PAMP-triggered immunity (PTI; Kim *et al.*, 2005; Tsuda *et al.*, 2013; Zipfel & Oldroyd, 2017).

Pattern recognition receptors include receptor-like kinases (RLKs) and receptor-like proteins (RLPs; Couto & Zipfel, 2016). Typical PRRs are composed of an extracellular domain, a transmembrane domain, and a kinase domain. The extracellular domains are variable ectodomains featuring leucine-rich repeats (LRRs), lysin motifs (LysMs), or lectin-type motifs. FLAGELLIN-SENSING 2 (FLS2) and the EF-Tu receptor (EFR) are established plant LRR-RLKs that perceive bacterial flagellin (or the epitope flg22) and elongation factor Tu (or the epitope elf18), respectively (Gomez-Gomez & Boller, 2000; Zipfel *et al.*, 2004, 2006). Likewise, the LysM-RLK, AtLYK5 and its co-receptor AtCERK1, form a complex that perceives chitin in *Arabidopsis thaliana* (Miya *et al.*, 2007; Wan *et al.*, 2008; Cao *et al.*, 2014). Upon perception of PAMPs, PRRs are activated and transduce the signal to downstream immune components, such as receptor-like cytoplasmic kinases (RLCKs). The *Arabidopsis* RLCK BOTRYTIS-INDUCED KINASE1 (BIK1) plays an important role downstream of PRRs. Lal *et al.* (2018) reported that EFR trans-phosphorylated BIK1 at the S89 and T90 residues and that phosphorylation of these two sites enabled BIK1 to localize to the nucleus and regulate the phosphorylation of WRKY transcription factors (TFs), triggering immune responses. In addition, BIK1 directly interacts with and phosphorylates RBOHD upon PAMP perception, which contributes to plant immunity by controlling the ROS burst and stomatal closure (Kadota *et al.*, 2014; Li *et al.*, 2014). *Arabidopsis* RLCK VII family members were recently shown to link multiple PRRs to MAPK activation. Specifically, RLCK VII kinases act downstream of PRRs to directly phosphorylate MAP kinase kinase kinase 5 (MAPKKK5), leading to the activation of MPK3/6 and defense

1 State Key Laboratory of Plant Genomics, Institute of Microbiology, Chinese Academy of Sciences, Beijing, China

2 CAS Center for Excellence in Biotic Interactions, University of Chinese Academy of Sciences, Beijing, China

3 College of Plant Protection, Fujian Agriculture and Forestry University, Fuzhou, China

4 Beijing Key Laboratory of Agricultural Product Detection and Control for Spoilage Organisms and Pesticides, Beijing University of Agriculture, Beijing, China

*Corresponding author. Tel: +86 10 6480 6131; E-mail: junliu@im.ac.cn

†These authors contributed equally to this work

gene expression (Bi *et al*, 2018; Rao *et al*, 2018). Thus, RLCKs play central roles in PRR-mediated plant immunity.

In addition to the PAMPs, flagellin, EF-Tu, and chitin, LPS is a key PAMP that activates immune responses in plants and animals (Dow *et al*, 2000; Silipo *et al*, 2010; Ranf *et al*, 2015; Ranf, 2016; Kagan, 2017). Lipopolysaccharide, an endotoxin that induces sepsis and septic shock in mammals, consists of an O-polysaccharide (OPS), core oligosaccharide, and the lipophilic lipid A, and is abundant in the outer membrane of Gram-negative bacteria (Ranf, 2016; Kagan, 2017). In mammals, LPS is recognized as a PAMP by extra- or intracellular LPS sensors. LPS binds to the TLR4/MD-2 receptor complex on the cell surface and triggers the expression of pro-inflammatory mediators (Poltorak *et al*, 1998; Shimazu *et al*, 1999; Park *et al*, 2009). By contrast, the TLR4-independent intracellular receptor caspase 11 perceives cytosolic LPS and activates the noncanonical inflammasome (Shi *et al*, 2014).

Although it has long been known that LPS activates immune responses in plants, the receptor of LPS was not identified yet. By screening the *Arabidopsis* mutants that are defective in the response to LPS, Ranf *et al* (2015) reported a G-type lectin RLK LORE (lipooligosaccharide-specific reduced elicitation), which belongs to a class of RLKs distinct from EFR/BAK1 or CERK1, is required for LPS-triggered immune responses. However, a recent study demonstrated that medium-chain 3-hydroxy fatty acids (mc-3-OH-FAs), but not LPS, are perceived by LORE during plant immunity (Kutschera *et al*, 2019). Free 3-OH-C10:0 has a binding affinity for the LORE ectodomain, suggesting that it is a ligand of LORE. Therefore, the previously reported LPS-activated immune responses were probably due to contamination by mc-3-OH-FAs or the structurally similar 3-hydroxy fatty acids (Kutschera *et al*, 2019).

Free mc-3-OH-FAs, which are released during lipid A biosynthesis, are widely present in *Pseudomonas* spp. (Kutschera *et al*, 2019). Furthermore, mc-3-OH-FAs are a group of key PAMPs that activate plant immunity in *Arabidopsis*. Although LORE is a key plant immune receptor for mc-3-OH-FAs, it is unknown how LORE is activated and what the downstream immune components are. Here, we report that the tyrosine 600 (Y600) residue of LORE is phosphorylated upon exposure to 3-OH-C10:0 and that the tyrosine-phosphorylated LORE then trans-phosphorylates specific RLCKs to transduce immune signals. In addition, we demonstrate that the bacterial tyrosine phosphatase HopAO1 inhibits the tyrosine phosphorylation of LORE, suppressing 3-OH-C10:0-activated immune responses. Our work clarifies the mechanism underlying LORE-mediated immune events in *Arabidopsis*, providing insight into an important plant immunity pathway.

Results

Tyrosine phosphorylation of LORE is essential for the 3-OH-C10:0-activated immune response

LORE harbors an extracellular lectin domain, a transmembrane domain, and a kinase domain (Ranf *et al*, 2015). The K516 and D613 residues of this RD (Arg-Asp) serine/threonine (S/T) kinase are conserved amino acids that are essential for its kinase activity (<https://www.uniprot.org/uniprot/O64782>). In order to investigate whether LORE possesses kinase activity, we purified the cytoplasmic domain of LORE (LORE-CD) fused to maltose-binding protein (MBP)

that had been heterologously expressed in *Escherichia coli*. *In vitro* kinase assays using ^{32}P -labeled adenosine triphosphate (ATP) showed that LORE is a *bona fide* kinase and that K516 and D613 are two essential sites for kinase activity, as recombinant LORE^{K516E} and LORE^{D613V} mutant proteins failed to undergo autophosphorylation (Fig EV1A).

We assessed the roles of kinase activity in LORE-mediated 3-OH-C10:0 perception using the kinase inhibitors tyrphostin A23 (A23) and K252a. K252a is a nonspecific kinase inhibitor of both S/T and tyrosine (Y) kinase activities, whereas A23 is a tyrosine kinase inhibitor (Macho *et al*, 2014). We treated *Arabidopsis* plants with K252a and A23 and examined them for ROS bursts triggered by 3-OH-C10:0. Both K252a and A23 strongly inhibited 3-OH-C10:0-triggered ROS bursts, and A23 abolished this response (Fig 1A). The inhibition of kinase activity and tyrosine phosphorylation also significantly reduced the transcript levels of PTI marker genes *FRK1* and *NHL10* (Fig 1B), suggesting that kinase activity and tyrosine phosphorylation are required for LORE-mediated PTI.

However, *in vitro* kinase assays using purified recombinant GST-LORE-CD protein showed the serine/threonine phosphorylation of LORE even when tyrosine phosphorylation was inhibited by A23 (Fig EV1B), revealing that LORE is a dual-specificity protein kinase. The observation that A23 completely suppressed the ROS burst triggered by 3-OH-C10:0 (Fig 1A) suggests that tyrosine phosphorylation is essential for LORE-mediated 3-OH-C10:0 recognition. To evaluate the role of tyrosine phosphorylation in LORE-mediated 3-OH-C10:0 recognition, we inhibited its phosphorylation using A23. MPK3/6 phosphorylation was markedly reduced (Figs 1C and EV1C). These observations highlight the critical role of tyrosine phosphorylation in LORE-mediated 3-OH-C10:0 recognition. Using an antibody that specifically recognizes phosphorylated tyrosine, we observed the 3-OH-C10:0-induced tyrosine phosphorylation of LORE *in planta*, but A23 inhibited this phosphorylation (Fig 1D).

Notably, the kinase activity of LORE is required for tyrosine autophosphorylation in recombinant proteins (Fig 1E). Using an anti-pY antibody, we detected the autophosphorylation of tyrosine in LORE recombinant protein, but mutations at K516 and D613 abolished this phosphorylation (Fig 1E). Furthermore, we introduced LORE, LORE^{K516E}, and LORE^{D613V} driven by the native LORE promoter into *Arabidopsis lore* mutants and detected tyrosine phosphorylation in plants harboring LORE, but not LORE^{K516E} or LORE^{D613V} (Fig EV1D). Thus, the kinase activity of LORE is required for tyrosine phosphorylation *in vitro* and *in vivo*.

3-OH-C10:0 induces phosphorylation of LORE at Tyr600

Using an *in vitro* kinase assay followed by liquid chromatography-tandem mass spectrometry (LC-MS/MS), we identified Y600 as a phosphorylation site in trypsin-digested LORE (Fig 2A; Appendix Table S1). Y600 is a conserved tyrosine site in G-type lectin kinases in *Arabidopsis* and rice (*Oryza sativa*; Fig EV2A). *In vitro* kinase assays revealed that the substitution of Y600 with phenylalanine (F; hereafter LORE^{Y600F}) markedly reduced the kinase activity of LORE (Fig 2B).

LORE Y600 is a conserved residue in many immunity-related RLK orthologous, including EFR, CERK1, and BAK1 (Fig EV2B; Macho *et al*, 2014; Liu *et al*, 2018; Perraki *et al*, 2018). To investigate the biological significance of Y600 phosphorylation, we generated and purified an antiserum that specifically detected Y600

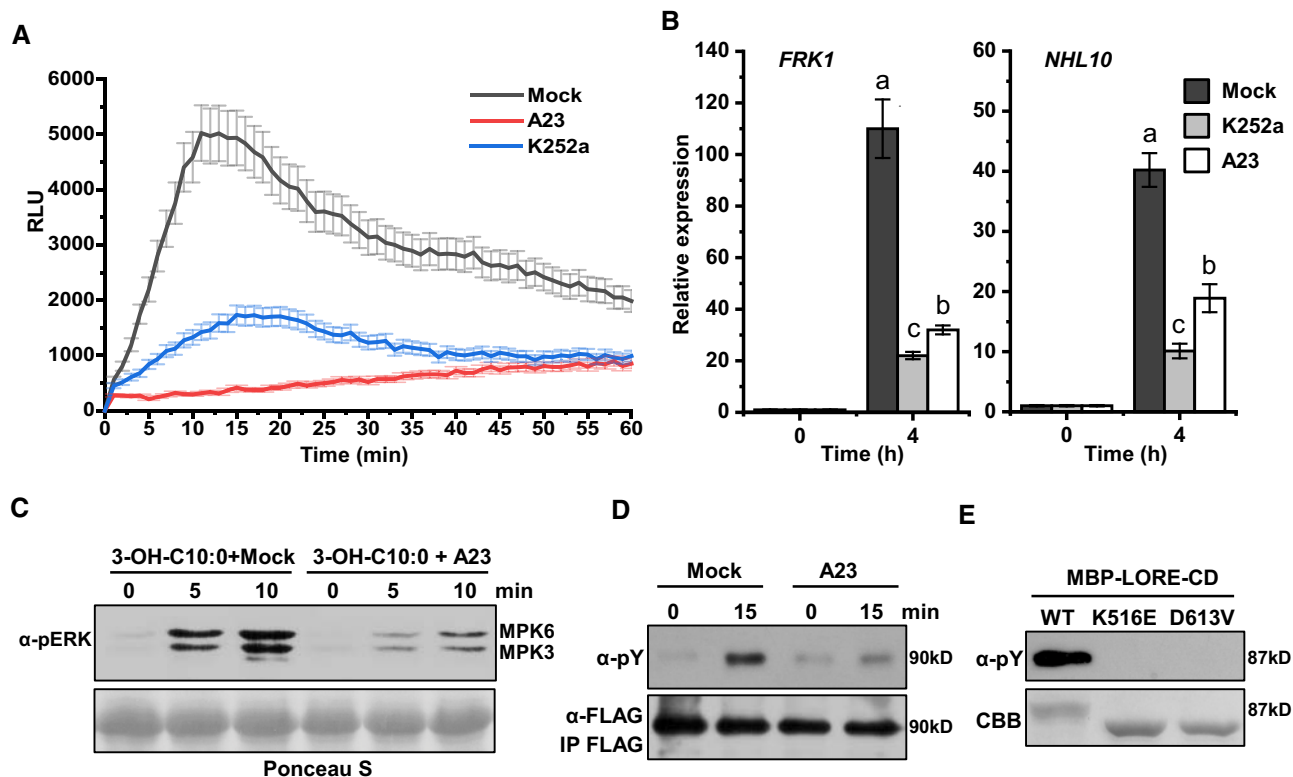


Figure 1. The kinase activity of LORE is essential for 3-OH-C10:0 sensing.

- A 3-OH-C10:0-induced ROS burst is suppressed by A23 and K252a. Two-week-old Col-0 seedlings were treated with 2 μ M K252a or 40 μ M A23. One hour later, 1 μ M 3-OH-C10:0 was used to trigger the ROS burst, and the photocount was recorded by a luminometer. Mock is solvent control. RLU, relative light unit. Values are means \pm SD ($n = 3$ biological replicates).
- B A23 and K252a suppress 3-OH-C10:0-induced PTI marker gene expression. Treatments with 3-OH-C10:0 and inhibitors were same as in (A), and the plant leaves were collected for RT-qPCR 4 h later. Values are means \pm SD ($n = 3$ biological replicates). ANOVA, $P < 0.01$.
- C MAPK cascade activation was inhibited by A23. Treatments with 3-OH-C10:0 and A23 were same as in (A). The plant leaves were collected at 0, 5, and 10 min for immunoblotting. Activated MAPKs were detected by immunoblotting with anti-phospho-p44/42 MAPK antibody. The corresponding bands are indicated for MPK3 and MPK6. Ponceau staining of Rubisco was used for estimating equal loading in each lane. The experiment was repeated three times with similar results.
- D Tyrosine phosphorylation of LORE *in vivo*. Two-week-old 35S:LORE-FLAG complementation plants were subjected to immunoprecipitation with anti-FLAG agarose beads. A23 (40 μ M) was used to inhibit the protein phosphorylation, and the treatments were same as in (A). Protein abundance of precipitated LORE-FLAG was detected by immunoblotting. The tyrosine phosphorylation was probed by anti-pTyrosine (α -pY) antibody. Similar results were observed in three biological replicates.
- E LORE is an active tyrosine kinase. The α -pY antibody was used to probe tyrosine phosphorylation in recombinant protein MBP-tagged LORE-CD (cytosolic domain). The LORE activation loop-conserved K516 was mutated to E, and D613 was mutated to V. The bottom gel showing protein abundance stained by Coomassie Brilliant Blue (CBB).

Source data are available online for this figure.

autophosphorylation in recombinant LORE-CD protein (Fig EV2C). Using this antiserum, we showed that LORE was indeed phosphorylated at Y600, whereas mutation at this site abolished its phosphorylation in planta (Fig 2C). Although LORE Y600 was phosphorylated at basal levels in these plants, 3-OH-C10:0 further promoted Y600 phosphorylation (Fig 2D). Notably, the phosphorylation level declined after 15 min (Fig 2D), suggesting that plant phosphatase(s) is(are) involved in regulating tyrosine phosphorylation.

LORE Y600 phosphorylation is required for LORE-mediated 3-OH-C10:0 recognition

Because 3-OH-C10:0 specifically induced Y600 phosphorylation in LORE, we investigated whether Y600 phosphorylation contributes to LORE-mediated recognition of 3-OH-C10:0. We complemented *lore*

mutant plants with LORE, LORE^{Y600F}, or the kinase-dead version, LORE^{K516E}, driven by the native LORE promoter. Semiquantitative RT-PCR revealed that these genes were expressed at similar levels in the transgenic plants (Fig EV2D). Consistent with a previous study, the *lore* mutants displayed significantly compromised ROS bursts in response to 3-OH-C10:0 (Kutschera *et al*, 2019; Fig 2E). Transformation with wild-type LORE fully complemented the aberrant phenotype of the *lore* mutant, whereas kinase-dead mutant LORE^{K516E} did not (Fig 2E). Similar to *pLORE:LORE^{K516E}*, the *pLORE:LORE^{Y600F}* complementation lines exhibited significantly reduced ROS levels. To rule out the possibility that the compromised ROS bursts in the *pLORE:LORE^{Y600F}* complementation lines resulted from altered protein abundance or mislocalization, we examined the protein stability of LORE^{Y600F} and demonstrated that it was as stable as LORE following 3-OH-C10:0 treatment (Fig EV2E). In addition,

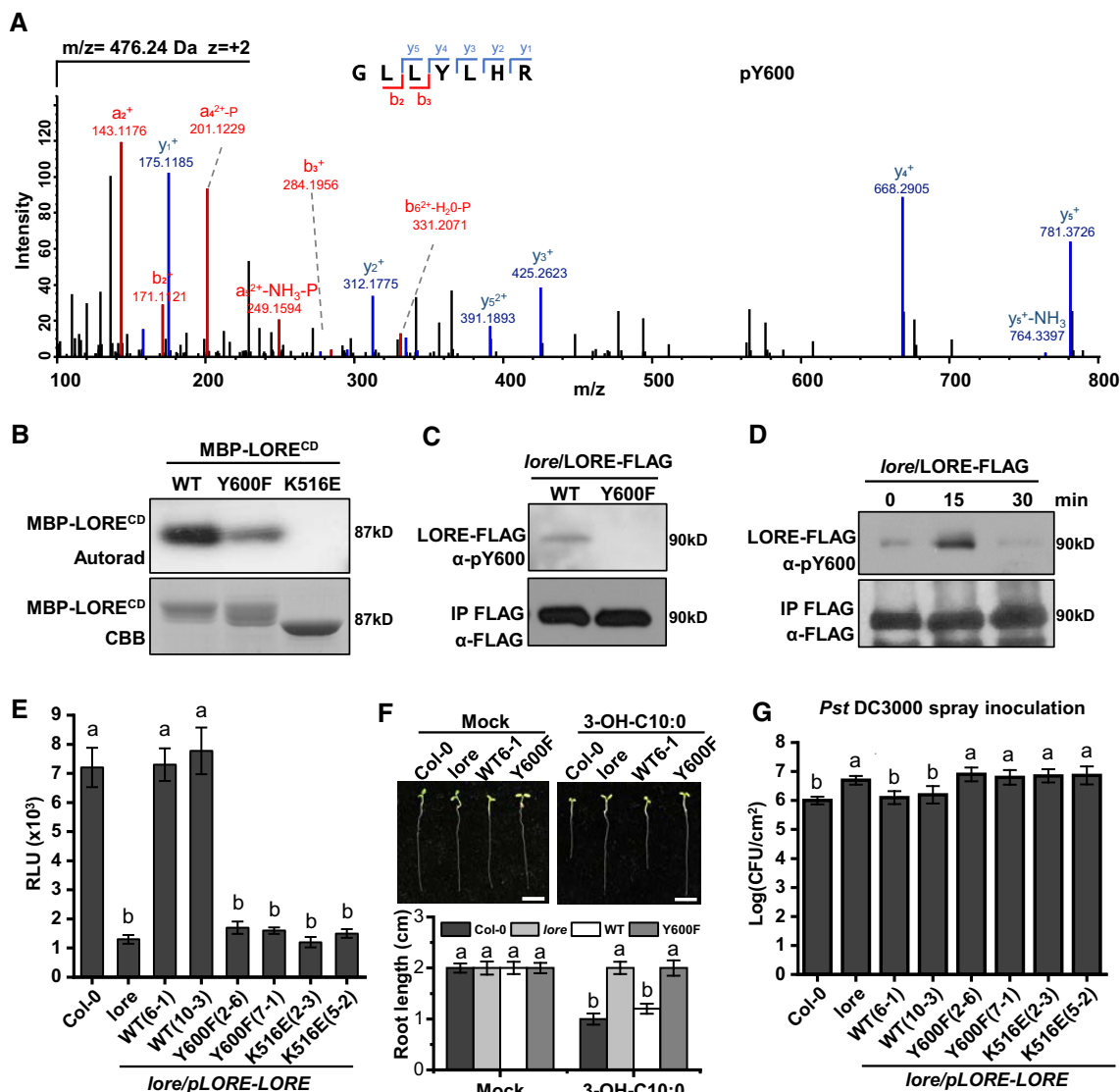


Figure 2. Y600 is a key phosphorylation site of LORE.

- A** Phosphorylated Y600 of LORE was identified by LC-MS/MS. MBP-tagged LORE-CD was used for *in vitro* kinase assays. Trypsin-digested recombinant proteins were subjected to LC-MS/MS analysis. The doubly charged peptide with m/z 476.24 matches GLLYLHR of LORE with Y600 phosphorylation. Fragment ions retaining charges in the N and C termini were denoted by “b” and “y”, respectively. pY600 indicated phosphorylated Y600.
- B** Y600 mutation reduced LORE kinase activity. MBP-tagged LORE-CD and LORE-Y600F-CD (Y600 tyrosine was substituted with phenylalanine, F) were subjected to kinase reactions. The kinase-dead mutant LORE^{K516E} served as a negative control. Autophosphorylated LORE was visualized by autoradiography following SDS-PAGE. Protein abundance was stained by CBB.
- C** LORE Y600 is phosphorylated in plants. Two-week-old *pLORE:LORE-FLAG* complementation plant leaves were subjected to immunoprecipitation (IP) with anti-FLAG agarose beads. Y600-specific phosphorylation antibody was used to detect Y600 phosphorylation in LORE. The experiment was repeated three times with similar results.
- D** 3-OH-C10:0 induced Y600 phosphorylation. Two-week-old *pLORE:LORE-FLAG* complementation plants were treated with $1 \mu\text{M}$ 3-OH-C10:0 at indicated times. Plant leaves were subjected to anti-FLAG IP. Phosphorylation level of Y600 was detected by anti-pY600 antibody. The experiment was repeated three times with similar results.
- E** Y600 mutation abolished the ROS burst triggered by 3-OH-C10:0. The transgenic plants were treated with 3-OH-C10:0, and ROS burst was measured. WT(6-1) and WT(10-3) are two independent complementation lines with LORE; Y600F(2-6) and Y600F(7-1) are two independent lines complemented with LORE^{Y600F}; and kinase-dead LORE^{K516E} was transformed to *lore* mutant as a negative control. The 2-3 and 5-2 are two independent lines. Values are means \pm SD ($n = 6$ biological replicates). ANOVA, $P < 0.01$.
- F** Y600 is required for growth inhibition by 3-OH-C10:0. The *Arabidopsis* seedlings were grown on $\frac{1}{2}$ MS containing $2.5 \mu\text{M}$ 3-OH-C10:0 for six days, and the root length was measured. The experiment was repeated three times with similar results. WT(6-1) and Y600F(2-6) lines were used for the assay. Scale bar = 0.4 cm. Values are means \pm SD ($n = 3$ biological replicates). ANOVA, $P < 0.01$.
- G** Y600 mutation decreased the disease resistance to *Pst* DC3000. Plants were spray-inoculated with *Pst* DC3000 at a concentration of 1×10^9 cfu/ml and were subjected to bacterial growth curve analysis at 3 dpi. Values are means \pm SD ($n = 6$ biological replicates). ANOVA, $P < 0.01$.

Source data are available online for this figure.

LORE^{K516E} and LORE^{Y600F} were also localized to the plasma membrane (Fig EV2F).

These observations suggest that Y600 phosphorylation is essential for LORE-mediated recognition of 3-OH-C10:0 and for PTI responses. To confirm this notion, we used RT-qPCR to examine the transcript levels of the PTI-responsive genes *FRK1* and *NHL10* in *Arabidopsis* leaves after 3-OH-C10:0 treatment. Indeed, these genes showed almost no response to 3-OH-C10:0 in the *pLORE:LORE^{Y600F}* complementation lines (Fig EV2G). The *pLORE:LORE^{Y600F}* complementation lines were as insensitive to 3-OH-C10:0 as the *lore* mutants in terms of growth inhibition, as indicated by their longer roots compared to Columbia-0 (Col-0) and the *LORE* complementation lines (Fig 2F).

Bacterial growth curve analysis revealed that Y600 is essential for LORE-mediated disease resistance. *pLORE:LORE^{Y600F}* complementation plants, similar to *pLORE:LORE^{K516E}* plants, exhibited enhanced disease susceptibility compared to Col-0 and *LORE* complementation plants (Fig 2G). As with other PAMPs (Zipfel et al, 2004, 2006; Cao et al, 2014), pretreatment with 3-OH-C10:0 enhances plant disease resistance (Kutschera et al, 2019). Therefore, we examined whether Y600 is required to prime defense responses. Pretreatment with 3-OH-C10:0 increased disease resistance in the *LORE* complementation lines, but not in the *pLORE:LORE^{Y600F}* complementation lines (Fig EV2H). These findings demonstrate that LORE Y600 phosphorylation is involved in signaling downstream of 3-OH-C10:0 perception.

LORE associates with PBL34 and its two paralogs

To further explore the downstream components of LORE signaling in *Arabidopsis*, we performed co-immunoprecipitation (co-IP) assays and searched the interacting proteins of LORE by LC-MS/MS in 2-week-old *35S:LORE-FLAG* transgenic *Arabidopsis* plants. We identified several potential LORE-interacting proteins using this strategy (Appendix Table S2). We focused on proteins that were predicted to localize to the plasma membrane or RLCKs, because RLCKs transduce PRR-mediated immune signals in plants (Bi et al, 2018). Among the LORE-interacting proteins identified, PBL34 (AT5G15080) satisfied the criteria (Appendix Table S2 and S3).

A yeast two-hybrid assay confirmed that PBL34 interacted with LORE-CD (Fig 3A). Because PBL34 has two close paralogs, PBL35 and PBL36, which belong to the same clade of the RLCK VII subfamily (Xu et al, 2017), we also tested their interactions with LORE. Both PBL35 and PBL36 interacted with LORE in yeast, but PBL39 did not, indicating that LORE interacts with specific PBLs (Fig 3A). We then employed several other approaches to validate this interaction. Using recombinant PBL proteins, we showed that MBP-PBLs successfully pulled down LORE-CD, but MBP alone did not (Fig 3B). In addition, by performing anti-FLAG co-IP and split-luciferase assays, we showed that PBLs interact with full-length LORE in *planta* (Fig 3C and D). By transiently expressing PBL34/35/36-GFP in *Nicotiana benthamiana* leaves via *Agrobacterium tumefaciens*-mediated transformation, we demonstrated that PBL34/35/36 localize to the plasma membrane (Appendix Fig S1A). Furthermore, we confirmed that LORE interacts with PBLs on the plasma membrane via BiFC assays in *N. benthamiana* (Appendix Fig S1B and C). These results suggest that PBL34/35/36 are components of the LORE complex that participate in LORE-mediated immune responses in *Arabidopsis*.

The *pbl34/35/36* mutant displays compromised responses to 3-OH-C10:0

As PBL34/35/36 belong to the same clade of the RLCK VII subfamily and associate with LORE, we investigated whether they participate in responses to 3-OH-C10:0 and are functionally redundant. *PBL34/35/36* were upregulated by treatment with 3-OH-C10:0 and *Pseudomonas syringae* pv. *tomato* (Pst) DC3000, with *PBL34* expressed at higher levels than *PBL35* and *PBL36*, as revealed by RT-qPCR (Fig EV3A). We then examined the PTI responses of the *pbl34,35,36* single mutants, the *pbl34/35* double mutant, and the *pbl34/35/36* triple mutant to 3-OH-C10:0. ROS burst assays showed that the responses of the *pbl34,35,36* single mutants to 3-OH-C10:0 were similar to those of Col-0, whereas the *pbl34/35* double mutant showed a slightly reduced response and the *pbl34/35/36* triple mutant showed a markedly reduced ROS burst (Fig 4A). We then examined two other PTI responses, namely *FRK1* and *NHL10* transcription and callose deposition, in the *pbl34/35/36* triple mutant. As shown in Fig 4B, the upregulation of *FRK1* and *NHL10* in response to 3-OH-C10:0 was significantly impaired in the *pbl34/35/36* triple mutant (Fig 4B). Likewise, the *pbl34/35/36* triple mutant accumulated much less callose than Col-0 (Fig 4C).

Next, we examined the effects of 3-OH-C10:0 on the growth of *pbl34/35/36*. Treatment with 3-OH-C10:0 strongly inhibited root growth in Col-0, but not in *lore* or *pbl34/35/36* (Fig 4D). Bacterial growth curve analysis supported the notion that the *pbl34/35/36* triple mutant exhibits compromised PTI, as the bacterial titer was significantly higher in the triple mutant, but not the *pbl34/35* double mutant, compared to Col-0; however, overexpression of PBL34 in Col-0 significantly enhanced disease resistance (Figs 4E and EV3B). In addition, pretreatment with 3-OH-C10:0 did not enhance the disease resistance of the triple mutant compared to Col-0 (Fig EV3C). Consistently, the overexpression lines showed higher ROS levels than Col-0 after 3-OH-C10:0 treatment (Fig EV3D). These results suggest that PBL34/35/36 are involved in the responses to 3-OH-C10:0 and are functionally redundant.

To further reinforce this notion, we complemented the *pbl34/35/36* triple mutant with *PBL34* driven by its native promoter, which completely restored the disease resistance phenotype to wild-type levels (Figs 4F and EV3E). Furthermore, the complementation lines exhibited a fully recovered ROS burst (Fig EV3F). Notably, unlike 3-OH-C10:0 whose induction of ROS burst was largely reduced in *pbl34/35/36* mutant, *flg22*, and chitin-induced ROS burst was only slightly compromised in the mutant when compared to their respective Col-0 controls (Fig EV3G). In addition, PTI marker gene transcript levels were not altered in the mutant (Appendix Fig S2A). However, 3-OH-C10:0-induced PTI responses were slightly reduced in *bik1/pbl1* mutant (Appendix Fig S2B and C). These results further indicate that the three PBLs are functionally redundant in LORE-mediated immune signaling and are specifically responsive to 3-OH-C10:0 than other PAMPs.

LORE phosphorylates PBL34

LORE is a *bona fide* kinase that interacts with PBL34 (Figs 3 and EV1). Therefore, we reasoned that LORE might phosphorylate PBL34 directly. *In vitro* kinase assays using recombinant proteins purified from *E. coli* demonstrated that GST-LORE-CD undergoes

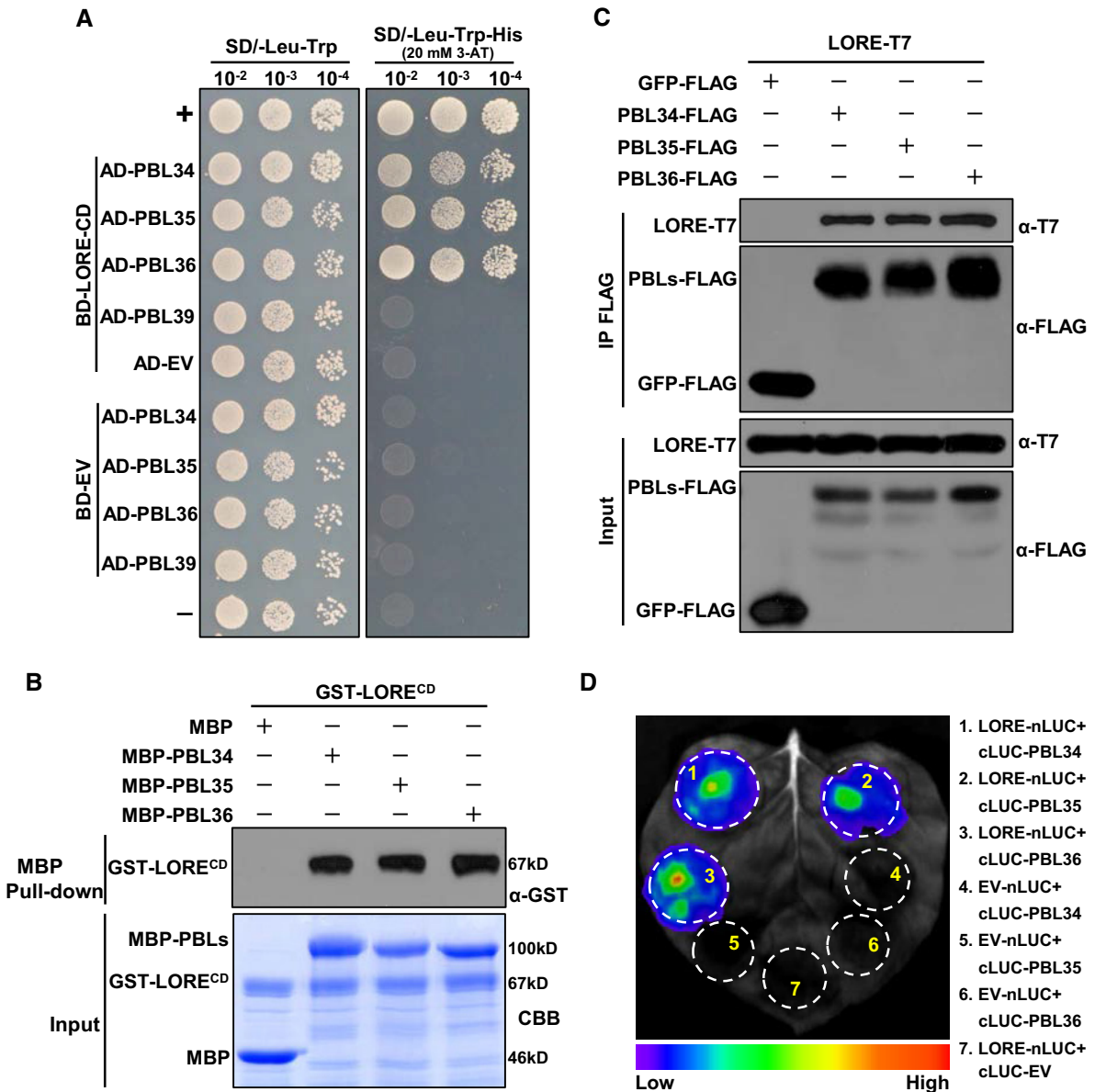


Figure 3. PBLs interact with LORE in vitro and in vivo.

A LORE interacts with specific RLCKs (PBL34/35/36) in yeast. BD-LORE-CD and AD-PBLs were co-transformed to yeast cells and were screened on synthetic dextrose media lacking leucine and tryptophan (SD/-Leu-Trp). The single yeast colonies were serially diluted onto SD/-Leu-Trp and SD/-Leu-Trp-His (SD media lacking leucine, tryptophan, and histidine) to observe yeast cell growth. 3-AT(20 mM) was used to inhibit the autoactivation of LORE. Yeast co-transformed with pGADT7-T+pGBKT7-53(+) served as a positive control, and the yeast co-transformed with pGADT7-T+pGBKT7-lam(-) and AD-PBL39 + BD-LORE served as the negative controls. EV, empty vector.

B LORE interacts with PBLs by MBP pull-down assays. The recombinant GST-LORE-CD and the MBP-PBLs were subjected to MBP pull-down analysis. MBP served as a negative control. The interacting proteins were revealed by anti-GST immunoblotting. The experiment was repeated three times with similar results.

C Co-immunoprecipitation (Co-IP) of LORE with PBLs. 35S promoter-driven LORE-T7 and PBLs-FLAG were transiently co-expressed in *N. benthamiana* by agroinfiltration. Plant leaves were immunoprecipitated with anti-FLAG beads, and the proteins were immunoblotted by anti-FLAG antibody. Co-IP proteins were immunoblotted by anti-T7 antibody. The experiment was repeated three times with similar results.

D LORE interacts with PBLs, revealed by split-luciferase assays. *N. benthamiana* leaves were co-infiltrated with Agrobacteria carrying 35S:LORE-nLUC and 35S:cLUC-PBLs. Images of chemiluminescence were obtained by applying 0.5 mM luciferin 36 h post-infiltration. Similar results were observed in three biological replicates.

Source data are available online for this figure.

autophosphorylation and directly phosphorylates MBP-PBL34, whereas the kinase-dead mutant protein GST-LORE^{K516E} does not (Fig 5A). An examination of the phosphorylation sites in PBL34 by

LC-MS/MS revealed that T306/T310 are phosphorylated by LORE-CD (Fig EV4A; Appendix Table S4). T306 and T310 are located at the conserved activation loop in many RLCK VII subfamily kinases

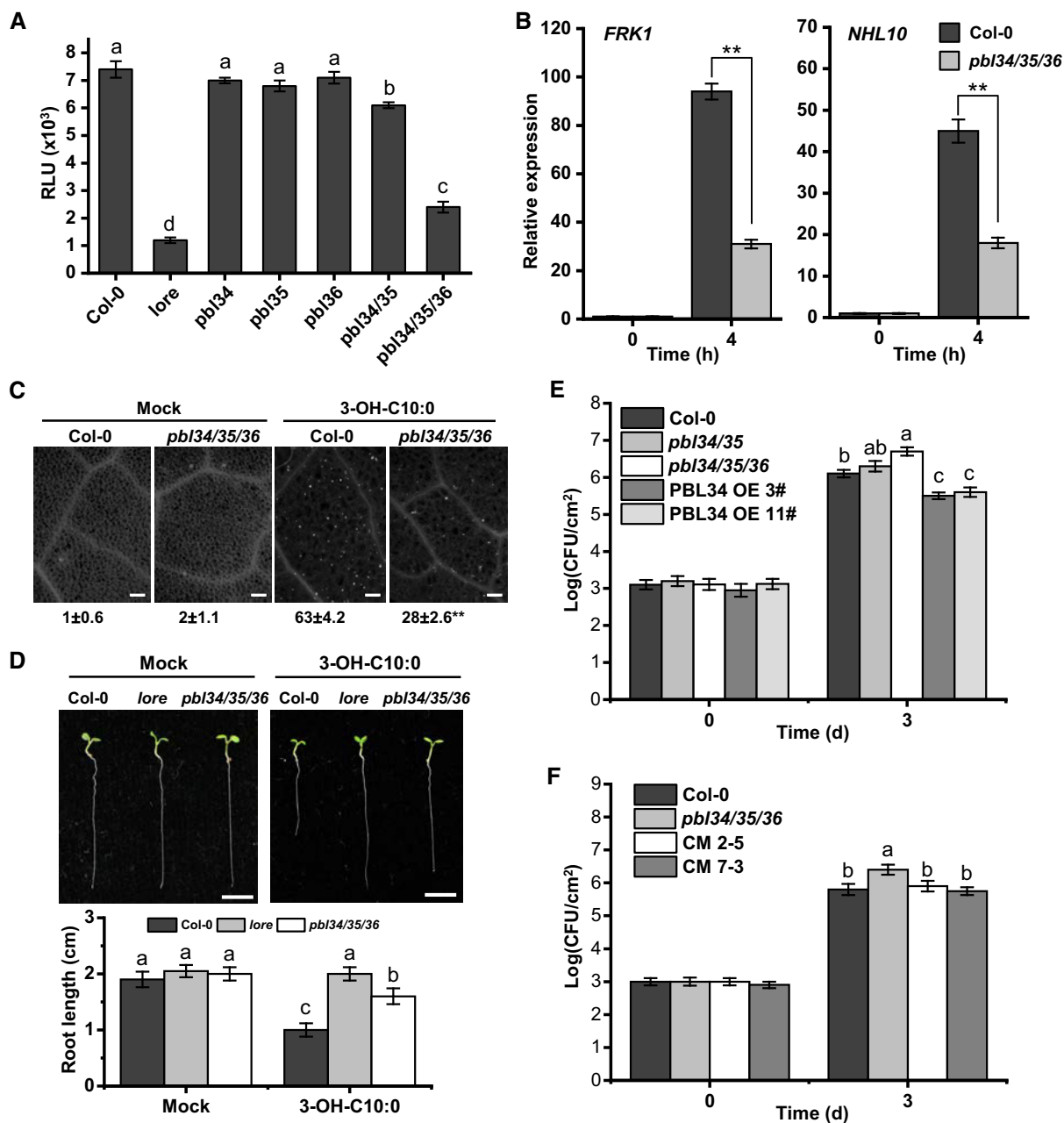


Figure 4. PBL triple mutants exhibited compromised PTI triggered by 3-OH-C10:0.

- A** ROS burst in *pbl34/35/36* triple mutant, induced by 3-OH-C10:0. Two-week-old seedlings were treated with 1 μ M 3-OH-C10:0, and the ROS burst was measured. Values are means \pm SD ($n = 6$ biological replicates). ANOVA, $P < 0.01$.
- B** PTI marker gene expression was reduced in *pbl34/35/36* triple mutant in response to 3-OH-C10:0. Treatment is same as in (A). Samples were collected for RT-qPCR at 4 h post-infiltration. Values are means \pm SD ($n = 3$ biological replicates). Student's t -test, ** $P < 0.01$.
- C** *pbl34/35/36* triple mutant displayed decreased callose depositions in response to 3-OH-C10:0 treatment. Two-week-old seedlings were sprayed with 1 μ M 3-OH-C10:0. The leaves were sampled for callose deposition assays 12 hrs later. The stained callose was counted for 1 mm² of the leaves. Mock is solvent control. Scale bar = 100 μ m. Values are means \pm SD ($n = 6$ leaves). Student's t -test, ** $P < 0.01$.
- D** Root length of *pbl34/35/36* triple mutant treated with 3-OH-C10:0. The *Arabidopsis* seedlings were grown on $\frac{1}{2}$ MS containing 2.5 μ M 3-OH-C10:0 for six days, and the root length was measured. Scale bar = 0.4 cm. Values are means \pm SD ($n = 3$ biological replicates). ANOVA, $P < 0.01$.
- E** Disease phenotype of *pbl34/35* double mutant, *pbl34/35/36* triple mutant, and PBL34 overexpression plants. *35S:PBL34-FLAG* was introduced to the Col-0 to generate the overexpression lines. The homozygous transgenic plants were used for the assays. The plants were sprayed with *Pst* DC3000 at a concentration of 1×10^9 cfu/ml. Plants were subjected to bacterial growth curve analysis at 3 dpi. OE-3# and OE-11# are two independent transgenic lines. Values are means \pm SD ($n = 6$ biological replicates). ANOVA, $P < 0.01$.
- F** *pbl34/35/36* triple mutant phenotype was rescued by PBL34. *PBL34-HA* was introduced to the triple mutant driven by its native promoter. Four-week-old homozygous seedlings were inoculated with 5×10^4 cfu/ml *Pst* DC3000, and the leaves were subjected to bacterial growth curve analysis at 3 dpi. CM2-5 and CM7-3 are two independent transgenic lines. Values are means \pm SD ($n = 6$ biological replicates). ANOVA, $P < 0.01$.

Source data are available online for this figure.

(Fig EV4B), suggesting that LORE-mediated phosphorylation of T306/T310 activates the kinase activity of PBL34.

To confirm that T306 and T310 are the major phosphorylation sites of PBL34, we mutated the two sites to alanine (PBL34^{T306A/T310A}, hereafter PBL34-2A). The mutations strongly diminished the radioactive signals of MBP-PBL34 in an *in vitro* kinase assay (Fig 5B), indicating that T306 and T310 are the two major sites in PBL34 that are phosphorylated by LORE. Notably, LORE^{Y600F} did not phosphorylate MBP-PBL34 as efficiently as wild-type LORE

(Fig 5C), indicating that the phosphorylation of PBL34 depends on the Y600 phosphorylation of LORE. We confirmed this by detecting S/T phosphorylation using a specific anti-pS/T antibody; GST-LORE-CD phosphorylated MBP-PBL34 more efficiently than LORE^{Y600F}-CD (Fig EV4C). The T306A and T310A mutations also impaired PBL34 kinase activity (Fig EV4D).

Since LORE phosphorylates the activation loop of PBL34 *in vitro* (Fig EV4B), we investigated whether this modification relies on LORE and whether 3-OH-C10:0 induces PBL34^{T306/T310}

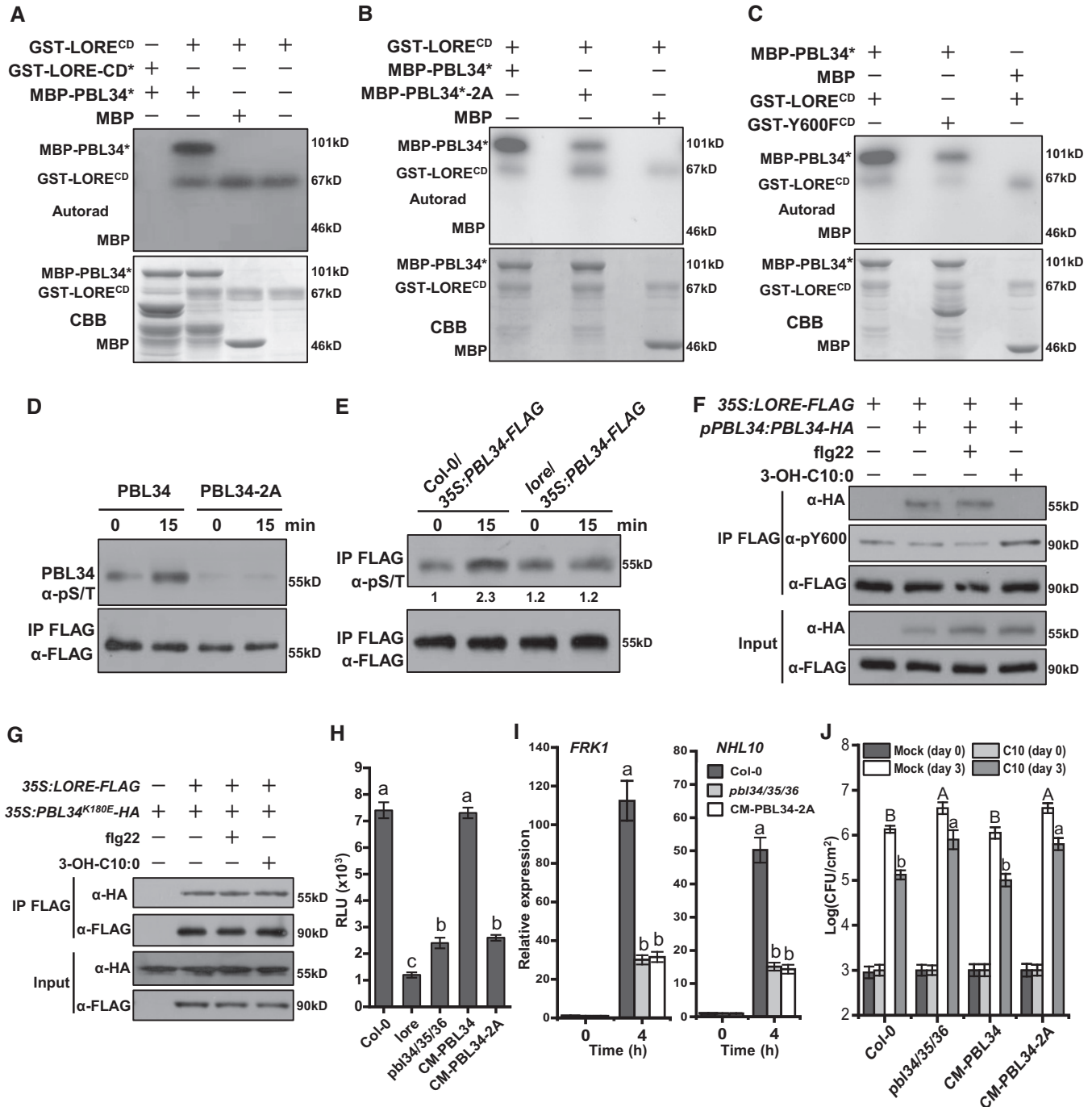


Figure 5.

Figure 5. LORE phosphorylates PBL34 at T306/T310 for immune responses.

- A PBL34 was phosphorylated by LORE *in vitro*. Purified recombinant proteins were used for *in vitro* kinase assays. The kinase-dead mutant MBP-PBL34* (PBL K180 was substituted to E, predicted by <https://www.uniprot.org/uniprot/>) was used as the substrate of GST-LORE-CD or its kinase-dead variant, GST-LORE-CD* (LORE^{K516E}). MBP served as a negative control. Incorporation of isotope-labeled phosphates was visualized by ³²P autoradiography. The CBB staining shows protein abundance.
- B Mutation of PBL34 T306/T310 significantly reduced its phosphorylation by LORE. Recombinant kinase-dead PBL34* and PBL34*-2A (T306/T310 was mutated to A) were incubated with LORE-CD. Phosphorylation of PBL34 was visualized by ³²P autoradiography. Protein abundance was revealed by CBB staining.
- C Mutation at Y600 diminished trans-phosphorylation activity of LORE. Recombinant LORE-CD and LORE^{Y600F}-CD were used for the trans-phosphorylation assays. Phosphorylation of PBL34 was visualized by ³²P autoradiography. Protein abundance was revealed by CBB staining.
- D PBL34 phosphorylation is induced by 3-OH-C10:0. The protoplast of Col-0 was transformed with 35S:PBL34-FLAG and 35S:PBL34-2A-FLAG, respectively. Sixteen hours later, the protoplasts were treated with 1 μM 3-OH-C10:0. Phosphorylated proteins were immunoprecipitated and detected by anti-pS/T antibody. The experiment was repeated three times with similar results.
- E 3-OH-C10:0-induced PBL34 phosphorylation depends on LORE. The 35S:PBL34-FLAG was introduced to Col-0 and *lore*, respectively. Four-week-old homozygous transgenic plants were treated with 1 μM 3-OH-C10:0. Phosphorylated proteins were immunoprecipitated and detected by anti-pS/T antibody. The experiment was repeated three times with similar results.
- F PBL34 dissociated from LORE upon 3-OH-C10:0 activation. The 35S:LORE-FLAG plants were transformed with native promoter-driven PBL34 (*pPBL34:PBL34-HA*), 100 nM flg22 or 1 μM 3-OH-C10:0 was sprayed onto plant leaves, and the leaves were sampled for assays 15 min later. The experiment was repeated three times with similar results.
- G Phosphorylation of PBL34^{K180E} did not disassociate from LORE. The 35S:LORE-FLAG protoplasts were transfected with 35S:PBL34^{K180E}-HA. 100 nM flg22 or 1 μM 3-OH-C10:0 was used to treat the protoplasts. The protoplasts were sampled 15 min later. The experiment was repeated three times with similar results.
- H PBL34 rescues *pbl34/35/36* triple mutant ROS burst in response to 3-OH-C10:0. Treatment was same as in (E). *pPBL34:PBL34-HA* was introduced to *pbl34/35/36* triple mutant, and the homozygous transgenic line was used for ROS burst assays. Values are means ± SD (*n* = 6 biological replicates). ANOVA, *P* < 0.01.
- I PTI marker gene expression in PBL34 complementation lines. The PTI marker gene *FRK1* and *NHL10* expression was examined by RT-qPCR in Col-0, *pbl34/35/36*, and *CM-PBL34-2A* lines after 3-OH-C10:0 treatments for 4 h. Values are means ± SD (*n* = 6; ANOVA; *P* < 0.01).
- J PBL34 phosphorylation at T306/T310 is essential for disease resistance. *pbl34/35/36* triple mutants were complemented with *PBL34* or *PBL34-2A* driven by its native promoter. The homozygous plants were pretreated with 3-OH-C10:0 (C10) 1 d before pathogen inoculation. The plants were inoculated with 2×10^5 cfu/ml *Pst* DC3000, and the bacterial titer was analyzed at 3 dpi. Mock is solvent control. Letters indicate the difference from Col-0. Values are means ± SD (*n* = 6; ANOVA, *P* < 0.01).

Source data are available online for this figure.

phosphorylation in *Arabidopsis*. We expressed PBL34 and PBL34-2A in *Arabidopsis* protoplasts, and then treated the protoplasts with 3-OH-C10:0. Phosphorylation of PBL34 was increased by 3-OH-C10:0 treatment, but that of PBL34-2A was not (Fig 5D), suggesting that T306/310 were phosphorylated in response to 3-OH-C10:0. We also transformed Col-0 and the *lore* mutant with *PBL34-FLAG* under the control of the 35S promoter. Treatment with 3-OH-C10:0 promoted the phosphorylation of PBL34 in Col-0 after 15 min. However, in the *lore* mutant background, the phosphorylation level of PBL34 was unchanged by 15 min of 3-OH-C10:0 treatment, as revealed using an anti-pS/T antibody (Figs 5E and EV4E). These observations suggest that the phosphorylation of PBL34 depends genetically on LORE and that 3-OH-C10:0 promotes this phosphorylation through LORE. Phosphorylated PBL34 dissociated from LORE, because PBL34 was immunoprecipitated by LORE in the absence of 3-OH-C10:0, whereas 3-OH-C10:0 (but not flg22) treatment facilitated the dissociation of PBL34 from LORE (Fig 5F). The 3-OH-C10:0-triggered dissociation of PBL34 from LORE is dependent on PBL34 kinase activity, because the kinase-dead variant of PBL34^{K180E} did not dissociate from LORE (Fig 5G). In addition to PBL34, PBL35 and PBL36 are also phosphorylated by LORE (Fig EV4F). These data suggest that LORE forms a complex with PBL34 or its PBL35 and PBL36 paralogs, but the complex dissociates in the presence of 3-OH-C10:0.

The phosphorylation of PBL34 at T306/T310 is essential for LORE-mediated recognition of 3-OH-C10:0

Because the T306/T310 phosphorylation of PBL34 genetically depends on LORE, we investigated the biological significance of this phosphorylation. Both T306 and T310 were required for the 3-OH-C10:0-mediated triggering of ROS bursts in *N. benthamiana*

(Fig EV4G). Therefore, we used PBL34-2A in subsequent experiments. In ROS burst assays, the *pbl34/35/36* triple mutant displayed reduced responses to 3-OH-C10:0; however, *PBL34* but not *PBL34-2A* rescued the ROS burst when transformed into the *pbl34/35/36* triple mutant background (Fig 5H). Notably, compared to *lore* or LORE(Y600F), *pbl34/35/36* and *PBL34-2A* were still weakly responsive to 3-OH-C10:0 treatment (Figs 5H and EV2H).

We also examined *FRK1* and *NHL10* transcript levels using RT-qPCR and demonstrated that transformation with *PBL34-2A* failed to rescue the reduced levels of these transcripts in *pbl34/35/36* plants in response to 3-OH-C10:0 (Fig 5I). These results indicate that the phosphorylation of PBL34 T306/T310 is required for 3-OH-C10:0-triggered PTI. Bacterial growth curve assays supported this conclusion, because *PBL34-2A* failed to rescue the susceptibility of *pbl34/35/36* to *Pst* DC3000 after pretreatment with 3-OH-C10:0 (Fig 5J). Furthermore, PBL34 phosphomimetic *CM-PBL34-2D* lines exhibited an enhanced ROS burst in response to 3-OH-C10:0 (Fig EV4H). These findings indicate that the phosphorylation of PBL34 T306/T310 by LORE is indispensable for 3-OH-C10:0-triggered immune responses.

LORE is targeted by the bacterial tyrosine phosphatase HopAO1

Pattern recognition receptors tyrosine phosphorylation has been reported in EFR and CERK1, and their phosphorylation is dynamically regulated by either the host or bacteria-delivered phosphatases (Macho *et al*, 2014; Liu *et al*, 2018). The *Pseudomonas*-secreted effector HopAO1 is a phosphatase that targets EFR, reversing tyrosine phosphorylation during the perception of EF-Tu and therefore leading to the suppression of PTI (Macho *et al*, 2014). We demonstrated that HopAO1 interacts with LORE-CD, as revealed by MBP and GST pull-down assays using recombinant proteins purified from

E. coli (Figs 6A and EV5A). Co-IP assays using transiently expressed proteins in *N. benthamiana* confirmed this interaction. As shown in Fig 6B, HopAO1-FLAG interacts with LORE-T7, whereas GFP-FLAG does not.

Because HopAO1 physically interacts with LORE, we examined whether it also dephosphorylates the phosphorylated tyrosine in LORE. Recombinant LORE is autophosphorylated in *E. coli*, as

revealed using a specific anti-pY600 antibody (Fig 6C). Indeed, recombinant HopAO1 but not the enzymatic mutant HopAO1^{CS} (Underwood *et al*, 2007) reduced the phosphorylation levels of Y600 in LORE in *in vitro* phosphatase assays. Similarly, co-expression of HopAO1 and LORE in *N. benthamiana* resulted in lower phosphorylation levels of Y600 in LORE compared with co-expression of LORE and GUS or HopAO1^{CS} (Fig 6D).

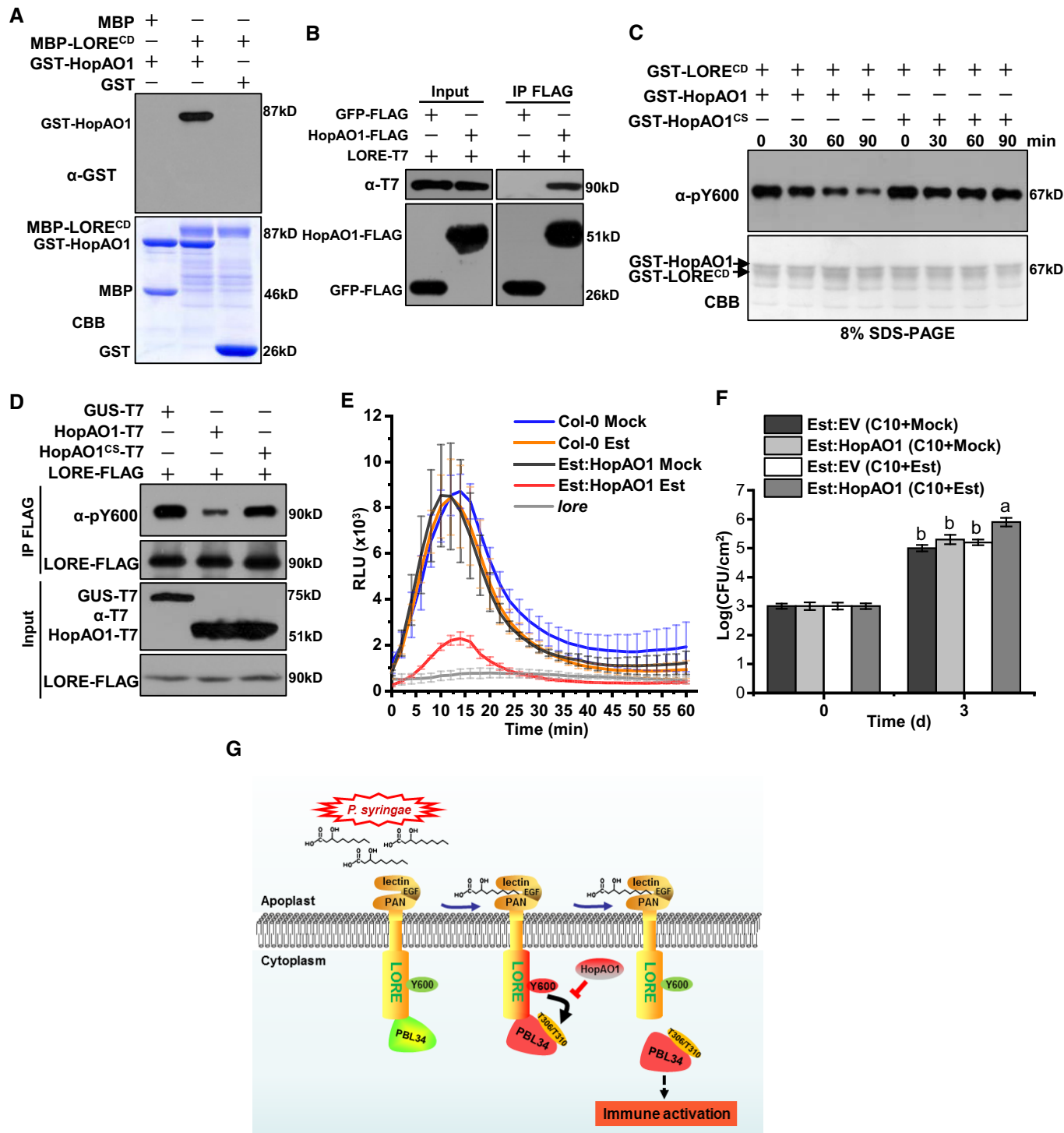


Figure 6.

Figure 6. *Pst* effector HopAO1 targets LORE for tyrosine dephosphorylation.

- A LORE interacts with HopAO1 by MBP pull-down assays. The recombinant GST-HopAO1 and the MBP-LORE-CD were subjected to MBP pull-down analysis. MBP and GST proteins served as the negative controls. The interacting proteins were revealed by anti-GST immunoblotting. The experiment was repeated three times with similar results.
- B LORE interacts with HopAO1 by Co-IP assays. 35S promoter-driven LORE-T7 and HopAO1-FLAG were transiently co-expressed in *N. benthamiana* by agroinfiltration. Plant leaves were immunoprecipitated with anti-FLAG beads and immunoblotted by anti-FLAG. Co-immunoprecipitated proteins were immunoblotted by anti-T7. The experiment was repeated three times with similar results.
- C HopAO1 dephosphorylates LORE Y600 *in vitro*. The recombinant GST-HopAO1/HopAO1^{CS} and GST-LORE-CD were subjected to *in vitro* phosphatase assays. Phosphorylation level of Y600 was detected by anti-pY600 immunoblotting. The experiment was repeated three times with similar results.
- D HopAO1 dephosphorylates LORE Y600 in *N. benthamiana*. LORE-FLAG was transiently co-expressed with GUS-T7, HopAO1-T7, or HopAO1^{CS}-T7 in *N. benthamiana* leaves mediated by *Agrobacterium*. The protein was immunoprecipitated and probed by anti-pY600 antibody. The experiment was repeated at least three times with similar results.
- E HopAO1 suppresses 3-OH-C10:0-triggered ROS burst. HopAO1 was ectopically expressed in Col-0 driven by estradiol-inducible promoter. 100 μ M estradiol was sprayed on *Est:HopAO1* plants, and the leaf disk was used for ROS burst assays 12 h later. Values are means \pm SD ($n = 6$ biological replicates).
- F HopAO1 inhibits 3-OH-C10:0-induced disease resistance. The *Est:HopAO1* plants were pretreated with 1 μ M 3-OH-C10:0 (C10) and 100 μ M estradiol, and then, the plants were inoculated with 5×10^4 cfu/ml *Pst* DC3000 24 h later. The bacterial titer was analyzed at 3 dpi. Values are means \pm SD ($n = 6$; ANOVA; $P < 0.01$).
- G Working model: LORE is phosphorylated at tyrosine 600 (Y600) at a basal level. In perception of 3-OH-C10:0, LORE Y600 phosphorylation is elevated, which then trans-phosphorylates PBL34 and likely its paralogs. Phosphorylated PBL34 dissociates from LORE, leading to immune activation. In this event, PBL34 kinase activity is required. However, the bacterial effector HopAO1 targets LORE Y600 and dephosphorylates the tyrosine-phosphorylated Y600, which subsequently suppresses immune response in *Arabidopsis*.

Source data are available online for this figure.

We also examined the role of HopAO1 during the LORE-mediated ROS burst triggered by 3-OH-C10:0. HopAO1 almost completely inhibited the ROS burst mediated by LORE in *Arabidopsis* or *N. benthamiana* leaves (Figs 6E, and EV5B and C). By contrast, functionally deficient HopAO1^{CS} did not inhibit this ROS burst (Fig EV5C and D). These results demonstrate that HopAO1 inhibits the ROS burst by dephosphorylating the tyrosine-phosphorylated Y600. In addition to reducing the ROS burst, HopAO1 also significantly decreased induction of the PTI marker genes (Fig EV5E). Consistently, transgenic *Arabidopsis* plants overexpressing HopAO1 driven by an estradiol-inducible promoter exhibited significantly compromised resistance to *Pst* DC3000 when pretreated with 3-OH-C10:0 after applying estradiol (Fig 6F). These results indicate that HopAO1 targets LORE, specifically dephosphorylating tyrosine-phosphorylated Y600 and therefore suppressing PTI.

Discussion

LORE is the first identified G-type lectin PRR shown to sense specific PAMPs, that is, mc-3-OH-FAs, in *Arabidopsis* (Kutschera et al, 2019). The discovery of mc-3-OH-FA as the ligand of LORE inspired us to investigate the signaling components involved in LORE-mediated immune responses. Indeed, one of the mc-3-OH-FAs, 3-OH-C10:0, specifically activated LORE in *Arabidopsis* (Figs 1 and 2). Although 3-OH-C10:0 and other mc-3-OH-FAs have not been shown to activate plant immunity in other plant species, mc-3-OH-FAs are undoubtedly another important type of PAMP, as they are widely present in Gram-negative bacteria and a part of lipid A, the major component of LPS (Kutschera et al, 2019). LPS is an important PAMP in mammalian immunity that also induces immune responses in plants, and intensive studies have aimed to identify its receptors in plants (Erbs & Newman, 2012). Future studies should investigate whether pure LPS (without mc-3-OH-FA contamination) can activate immune responses in other plants, although only free mc-3-OH-FA activates immunity in *Arabidopsis*. Indeed, treatment with *Xylella fastidiosa* LPS O-antigen delayed plant innate immune recognition in grapevine (Rapicavoli et al, 2018),

implying that plants recognize LPS through other moiety in addition to mc-3-OH-FAs.

Upon 3-OH-C10:0 treatment, we observed tyrosine phosphorylation of LORE, which is required for LORE-mediated PTI (Fig 1). Furthermore, we identified a key autophosphorylation site at Y600, which is conserved in all G-type lectin RLKs (Figs 2A and EV2A). LORE Y600 is a conserved residue in many immunity-related RLKs, including EFR, CERK1, and BAK1 (Fig EV2B), which are important for PTI signaling (Macho et al, 2014; Liu et al, 2018; Perraki et al, 2018). The kinase activity assays revealed that LORE is a dual-specificity protein kinase and that tyrosine kinase activity is required for the 3-OH-C10:0-triggered immune response (Fig EV1). LRR-RLK EFR and Lys-motif RLK CERK1 were previously characterized as tyrosine kinases whose key phosphorylation sites are Y836 and Y428, respectively (Macho et al, 2014; Liu et al, 2018). Here, we report that the lectin RLK, LORE, is a dual-specificity protein kinase and that the phosphorylation of Y600 of LORE is required for 3-OH-C10:0-triggered ROS production and resistance to *Pst* DC3000, highlighting the critical roles of LORE Y600 (Fig 6G).

Unlike animal PRRs, which often associate with cytoplasmic kinases through adaptor proteins (Ausubel, 2005), plant PRRs transduce signals by directly phosphorylating their downstream substrates (Tang et al, 2017). In plants, the eATP receptor kinase DORN1 (Does not Respond to Nucleotides 1) is a well-known immune-related lectin RLK. DORN1 phosphorylates the NADPH oxidase RbohD to produce ROS extracellularly, thereby controlling stomatal immunity to restrict *Pst* DC3000 invasion (Chen et al, 2017). However, PRRs often trans-phosphorylate RLCKs to transduce immune signaling in plants. Many RLCKs phosphorylate downstream immune proteins; for example, upon activation by flg22, BIK1 and PBL1 phosphorylate RbohD at multiple sites required for ROS production (Kadota et al, 2014; Li et al, 2014). Following the perception of EF-Tu, EFR phosphorylates the RLCK BIK1, and the phosphorylated BIK1 localizes to the nucleus to regulate WRKY TF-mediated immunity (Lal et al, 2018). During fungal pathogen invasion, the LysM-RLK LYK5 cooperates with CERK1 to recognize chitin and subsequently activates RLCK VII-4 subfamily members, which further phosphorylate the MAPK cascade, leading

to immune responses (Bi *et al*, 2018). These observations suggest that PRRs transduce immune signaling via RLCKs.

Accumulating evidence indicates that phosphorylation of PRR key tyrosine sites is required for downstream RLCK activation. Treatment of plants with the tyrosine kinase inhibitor tyrphostin A23 demonstrated that tyrosine phosphorylation is important for PTI responses (Macho *et al*, 2014). elf18-dependent tyrosine phosphorylation of EFR is essential for the activation of EFR; specifically, the phosphorylation of Y836 is required to activate EFR and downstream RLCK BIK1 phosphorylation (Macho *et al*, 2014). Notably, tyrosine phosphorylation is also essential for BAK1 function in immune signaling (Perraki *et al*, 2018). BAK1 is a co-receptor for many LRR-RKs and functions in plant immunity, growth, and development (de Oliveira *et al*, 2016; Yamada *et al*, 2016; Peng *et al*, 2018; Zhou *et al*, 2019). A recent study showed that Y403 phosphorylation is required for BAK1 function in immune signaling, highlighting the importance of tyrosine phosphorylation for this immune protein (Perraki *et al*, 2018). In addition, BAK1 phosphorylates BIK1 at tyrosine and serine/threonine residues, and tyrosine and serine/threonine kinase activities are crucial for BIK1 function, emphasizing the importance of the tyrosine phosphorylation cascade in plant immunity (Lin *et al*, 2014). Similar to EFR, CERK1 Y428 phosphorylation is indispensable for chitin-triggered activation of CERK1 and its dynamic interaction with downstream RLCKs (Liu *et al*, 2018). Notably, CERK1 Y557 phosphorylation is required for the chitin-triggered dissociation of CERK1 from BIK1 (Liu *et al*, 2018).

In this study, using immunoprecipitation assays, we determined that LORE interacts with and phosphorylates three RLCK paralogs: PBL34/35/36 (Figs 5 and EV4). Rao *et al* (2018) showed that RLCK VII members are specifically involved in signaling pathways downstream of multiple PRRs. PBL34/35/36 were timely induced by 3-OH-C10:0 (Fig EV3A), underpinning their roles in LORE-mediated immunity. It is worth to mention that we did not find additional RLCKs in the assays, suggesting that LORE might not require a co-receptor, in contrast to other known LRR- or LysM-type PRRs reported to date (Couto & Zipfel, 2016). We confirmed that LORE phosphorylates the conserved activation loops of these PBLs and that the phosphorylation sites T306 and T310 are critical for 3-OH-C10:0-triggered immunity. Similar to PBL34/35/36, phosphorylation of the BIK1 activation loop by BAK1 is required for flg22 perception (Lu *et al*, 2010). Notably, Y600 phosphorylation is induced by 3-OH-C10:0, which might be crucial for PBL34/35/36 phosphorylation/activation (Fig 5). Similar to this observation, BIK1 is activated upon EFR-mediated recognition for EF-Tu perception (Macho *et al*, 2014; Perraki *et al*, 2018). Following the phosphorylation of PBL34/35/36 by LORE, these proteins, which might form a complex with LORE separately, dissociate from LORE, and the dissociation is dependent on the activity of PBL kinases (Fig 5F and G). Likewise, during flg22 recognition, active FLS2-BAK1 trans-phosphorylates BIK1, which is then released from the FLS2-BAK1 complex to activate intracellular signaling (Lu *et al*, 2010). Notably, in addition to PBL34/35/36, BIK1 appears to be weakly involved in 3-OH-C10:0-triggered PTI responses (Appendix Fig S2B and C). Whether BIK1 plays a similar role as that in FLS2-BAK1 module needs further investigation. Nevertheless, the critical role of PBL34 kinase activity is not depicted in this model (Fig 6G). We speculate that PBL34 phosphorylates another protein(s), which contributes to the

dissociation. Alternatively, PBL34 autophosphorylation might also contribute to the disassociation from LORE.

Bacterial pathogens subvert plant immunity by interfering with immune signal transduction (Jones & Dangl, 2006). The bacterial tyrosine phosphatase HopAO1 targets and dephosphorylates EFR and therefore interferes with immune responses (Macho *et al*, 2014). Here, we demonstrated that HopAO1 interacts with and dephosphorylates tyrosine-phosphorylated Y600 of LORE, resulting in compromised 3-OH-C10:0-activated ROS production (Fig 6). These results indicate that a *Pst*-secreted effector targets plant LecRLKs and suggest that HopAO1 might also target the tyrosine residue of other PRRs to suppress immune responses. Nevertheless, 3-OH-C10:0-induced LORE Y600 phosphorylation peaked at 15 min but declined at 30 min (Fig 2D), suggesting the existence of a dephosphorylation machinery that removes LORE phosphorylation. Indeed, the plant phosphatase CIPP1 reverses the tyrosine phosphorylation of CERK1 upon chitin elicitation (Liu *et al*, 2018). Future studies should investigate how *Arabidopsis* plants dynamically regulate the tyrosine phosphorylation of LORE during 3-OH-C10:0 perception.

The discovery of mc-3-OH fatty acids as important PAMPs of Gram-negative bacteria should facilitate the exploration of their receptors in other plants. Such studies might also elucidate the roles of pathogen-carried fatty acids as immune activators, which might be perceived by LORE or other lectin RLKs. This study revealed the importance of a conserved tyrosine residue of LORE and its downstream signaling components for LORE-mediated recognition of 3-OH-C10:0. Future studies should investigate whether the activation of LORE and its downstream RLCKs is similar to other lectin RLK-mediated immune responses, especially for fatty acid types of PAMPs. In summary, we discovered that LORE-mediated recognition of 3-OH-C10:0 occurs via tyrosine phosphorylation and demonstrated that PBL34/35/36 are key RLCKs that function downstream of LORE to regulate plant immunity; however, *Pst* DC3000 deploys an effector HopAO1 that inhibits tyrosine phosphorylation, which subverts plant immunity.

Materials and Methods

Plant materials and growth conditions

Arabidopsis thaliana lore (SAIL_857_E06), *pbl34* (SALK_067743), *pbl35* (SALK_039402), and *pbl36* (SAIL_885_B03) T-DNA knockout lines were obtained from the *Arabidopsis* Biological Resource Center. Plants were grown at 23°C under 10 h of light/14 h of dark for 4 weeks. For ROS measurement and MAPK assays, 2-week-old seedlings were used. Transgenic plants were generated via floral dip transformation procedure (Clough & Bent, 1998).

To generate the *LORE-FLAG* overexpression plant, the *LORE* coding sequence was cloned into pMD-1 binary vector driven by a *CaMV* 35S promoter. For the generation of *LORE* complement plants, the genomic DNA of *LORE* and its native promoter was cloned into pGWB13 vector. Point mutation of *LORE* was introduced by overlap extension PCR with primers as listed in Appendix Table S5. Constructs were verified by sequencing and introduced to *Agrobacterium tumefaciens* strain GV3101 by electroporation. The overexpression plants and complementation plants

were selected with 25 µg/ml kanamycin and 25 µg/ml hygromycin, respectively. The double and triple mutants of *PBLs* were generated by crossing. To complement *pbl34/35/36* triple mutants, the genomic DNA of *PBL34* and its native promoter was cloned into pGWB13 vector. Point mutation of *PBL34* was introduced by overlap extension PCR. The complementation plants were selected using 25 µg/ml hygromycin.

Pathogen inoculation assay

Pseudomonas syringae pv. *tomato* (*Pst*) DC3000 was grown on NYGA medium for 2 days at 28°C. For syringe inoculation, 5-week-old plants leaves were infiltrated with 5×10^4 cfu/ml *Pst* DC3000 in 10 mM MgCl₂. For spray inoculation, 5-week-old plants were sprayed with 1×10^9 cfu/ml *Pst* DC3000. The bacterial titers were determined by growth curve analysis as described by Liu *et al* (2011). Callose deposition assays were performed as described by Gimenez-Ibanez *et al* (2009). Briefly, the 3-OH-C10:0-treated plant leaves were sampled at 12 h and the whole leaves were immersed in 5 ml of alcoholic lactophenol (phenol: glycerol: lactic acid: water mixed with equal volume) at 65°C for 15 min to clear chlorophyll. The cleared leaves were stained by 0.01% aniline blue in 150 mM K₂HPO₄ for 30 min. The stained callose was examined by epifluorescence illumination.

ROS burst measurement

Two-week-old *Arabidopsis* seedling leaves were sampled for leaf disks and kept in 96-well plate with ddH₂O overnight. Before measurement, ddH₂O was replaced by reaction mixtures containing 17 mM luminol L-012 (Wako), 10 mg/ml horseradish peroxidase, and 1 µM 3-OH-C10:0. Each treatment contained at least six replications. Luminescence was measured continuously for 60 min with a Centro XS3 LB 960 (Berthold Technologies). In the experiment with kinase inhibitors, K252a or A23 was applied to plant leaves for 1 h before ROS measurement.

MAPK assay

Two-week-old *Arabidopsis* seedling leaves were sprayed with 1 µM 3-OH-C10:0 (Matreya LLC). Samples were collected and frozen in liquid nitrogen at indicated time points. Total proteins were extracted with 3 × Laemmli buffer containing 1 × EDTA-free protease inhibitor and 1 × Phosphatase Inhibitor Mini Tablets (Thermo Fisher Scientific, USA). The soluble total protein was separated on a 12% SDS-PAGE. Activated MAPKs were detected by anti-PERK antibodies (Cell Signaling Technology Inc.).

Quantitative RT-PCR

Arabidopsis leaves were collected in 1.5-ml RNase-free centrifuge tubes at indicated time points. Total RNA was extracted using TRIzol (Invitrogen). RNA concentration was determined with a NanoDrop 2000. One microgram of RNA was subjected to reverse transcription by HiScript Q RT SuperMix for qPCR with genomic DNA wipe according to the manufacturer's instructions (Vazyme, China). ChamQ SYBR qPCR Master Mix (Vazyme, China) was used for quantitative RT-PCR. Reactions were detected by the Bio-Rad

system. *ACTN2* was used as an internal control. Primers are listed in Appendix Table S5.

Yeast two-hybrid assays

Yeast experiments were conducted according to the manufacturer's protocol (Matchmaker, Clontech). The coding sequence of LORE was cloned into pGBKT7, and *PBL34*, *PBL35*, *PBL36*, and *PBL39* were cloned into pGADT7. pGADT7-T and pGBKT7-53 were used as positive controls. pGADT7-T and pGBKT7-lam served as a negative control. Co-transformed yeast cells were screened on synthetic dropout media lacking leucine and tryptophan (SD/-Leu-Trp). The single yeast colonies were serially diluted onto SD/-Leu-Trp and SD/-Leu-Trp-His to observe yeast cell growth. 3-AT (20 mM) was added to SD/-Leu-Trp-His to inhibit the autoactivation of LORE.

MBP pull-down assay

LORE's cytoplasmic domain was cloned into pGEX-4T to generate GST-LORE-CD. *PBL34*, *PBL35*, *PBL36*, and HopAO1 were cloned into pMAL-C4X or pGEX-4T to generate MBP-*PBL34*, MBP-*PBL35*, MBP-*PBL36*, and GST-HopAO1, respectively. Protein purification and MBP pull-down assays were performed as described by Liu *et al* (2011).

Co-IP and immunoblotting analysis

Co-IP in *Nicotiana benthamiana* was performed according to the method described by Luo *et al* (2017). For Co-IP in *Arabidopsis*, homozygous plants overexpressing *LORE-FLAG* were transformed into *pPBL34:PBL34-HA*. Plants co-expressing *LORE-FLAG* and *PBL34-HA* were grown in one-half-strength Murashige and Skoog (MS) medium for 10 days. Plant seedlings (0.5 g) were ground in liquid nitrogen and extracted in extraction/wash buffer containing 50 mM Tris-HCl (pH 7.5), 150 mM NaCl, 0.1% Triton X-100, 0.2% Nonidet P-40, 1 mM DTT, 1 × complete protease inhibitor (Roche), and 1 × phosphatase tablet (Roche). The homogenate was centrifuged at 15,000 g for 20 min. Anti-Flag antiserum-conjugated agarose beads (Sigma) were added to the supernatant. After incubation in 4°C on an end-over-end shaker for 1.5 h, the beads were spun down at 1,500 g for 2 min and washed with wash buffer at least five times. The bound proteins were eluted by 1.5 × Laemmli loading buffer, resolved by 12% SDS-PAGE, and subjected to immunoblot analysis.

Confocal microscopy

For subcellular localization, GFP-tagged LORE and *PBLs* were transiently expressed in *N. benthamiana* and observed using a confocal laser microscope (Leica model TCS SP8). The excitation wavelengths and emission filters were 488 nm and band-pass 500–550 nm, respectively.

pSAT1-nYFP and pSAT1-cYFP plasmids were used for the BiFC assays. LORE was cloned into pSAT1-cYFP at the C terminus. *PBL34*, *PBL35*, *PBL36*, and *PBL39* were cloned into pSAT1-nYFP. The constructs were transformed into *A. tumefaciens* strain C58C1 and transiently expressed in *N. benthamiana*. The

fluorescence was observed using a confocal laser microscope (Leica Model TCS SP8) 36 hpi before cell death. The excitation wavelength and emission filter were 514 nm and band-pass 530–560 nm, respectively.

Phosphosite antibody preparation

Phosphosite-specific antibodies were generated at Abmart Inc. Briefly, the phosphopeptide RGLL(pY)LHRDSC and control peptide RGLLYLHRDSC were synthesized and conjugated to keyhole limpet hemocyanin (KLH) carrier. Four rabbits were immunized by the conjugated phosphopeptide. Affinity chromatography with phosphopeptides was used to purify the polyclonal antiserum. The nonspecific antibody was removed by affinity chromatography with control peptides. The Y600 phosphosite-specific antibody was diluted by 1:300 for immunoblotting.

In vitro kinase activity assays

The *in vitro* kinase activity assays were performed according to the method described by Liu *et al* (2011) with slight modifications. Protein expression in *Escherichia coli* was induced with 0.5 mM IPTG for 12 h at 16°C. Purified proteins were incubated in 30 µl kinase buffer containing 20 mM Tris–HCl (pH 7.5), 10 mM MgCl₂, 1 mM CaCl₂, 10 µM ATP, 1 mM DTT, 2 µg kinase, and 1–2 µg recombinant protein as substrates. For ³²P isotope-labeled reactions, assays were initiated by adding 1 µl (10 µCi) ³²P-ATP and incubated for 45 min at 30°C. Denatured proteins were separated on an 8% SDS–PAGE, and phosphorylated proteins were visualized by X-ray film exposure. For kinase assays only with cold ATP, 30 µl kinase buffer contained 20 mM Tris–HCl (pH 7.5), 10 mM MgCl₂, 1 mM CaCl₂, 1 mM ATP, 1 mM DTT, 2 µg kinase, and 1–2 µg recombinant protein as substrates and incubated for 45 min at 30°C. Denatured proteins were separated on 8% SDS–PAGE, and phosphorylated proteins were detected by anti-pTyr (Sigma, P5872) or anti-pSer/Thr antibodies (ECM Bioscience, PP2551). The secondary antibodies are HS201-01 (goat anti-mouse) and HS101-01 (goat anti-rabbit) from TransGen Biotech.

LC-MS/MS analysis

To identify autophosphorylation sites of LORE, 10 µg of recombinant MBP-tagged LORE-CD proteins was incubated in kinase buffer containing 1 mM ATP for 70 min at 30°C. To identify phosphorylation sites of PBL34 by LORE-CD, 10 µg of recombinant MBP-tagged LORE-CD proteins was incubated with 5 µg GST-tagged PBL34 in kinase buffer containing 1 mM ATP for 70 min at 30°C. The kinase reactions were terminated by adding 3 × Laemmli buffer and then incubated at 95°C for 5 min. Denatured proteins were separated by 8% SDS–PAGE and subjected to trypsin digestion. Phosphopeptides were analyzed by the Q Exactive LC-MS/MS system (Thermo Scientific, Beijing Qinglian Biotech Co., Ltd). Spectra were analyzed by MaxQuant software, and phosphorylation sites were confirmed manually.

In vitro phosphatase assay

The phosphatase assay was conducted according to the method described by Macho *et al* (2014) with some modifications. Briefly,

3 µg GST-tagged HopAO1 was incubated with 2 µg GST-tagged LORE in phosphatase buffer at 30°C for 60 min, and 3 × Laemmli buffer was added to terminate the reaction. Denatured proteins were separated by 8% SDS–PAGE, and pY600 antibody was used to detect the phosphorylation level of GST-LORE.

Statistical analysis

All the data were analyzed using two-tailed Student's *t*-test or one-way ANOVA with SPSS 18.0. The values represented as means ± standard deviation (SD).

Data availability

Sequence data from this article can be found in the GenBank/EMBL database under accession numbers LORE (At1g61380), PBL34 (At5g15080), PBL35 (At3g01300), PBL36 (At3g28690), FRK1 (At2g19190), and NHL10 (At2g35980).

Expanded View for this article is available online.

Acknowledgments

We thank Prof. Jie Zhang at Institute of Microbiology, Chinese Academy of Sciences, for providing the *bik1/pbl1* seed. We also thank Prof. Gitta Coaker and Prof. Savithramma P. Dinesh-Kumar at University of California, Davis, for reading the manuscript. The study was supported by the National Key R&D Program of China (2017YFD0200900), the Chinese Academy of Sciences (Strategic Priority Research Program Grant No. XDB11020300), Natural Science Foundation of China (31570252, 31601629), start-up funding from the “One Hundred Talents” program of the Chinese Academy of Sciences, and a grant from the State Key Laboratory of Plant Genomics (Grant No. O8KF021011) to JL.

Author contributions

JL and XL conceived and designed the experiments; XL, WW, YL, and NX performed most of the experiments; ZW and HZ provided technical assistance; JL and XL wrote the article.

Conflict of interest

The authors declare that they have no conflict of interest.

References

- Ausubel FM (2005) Are innate immune signaling pathways in plants and animals conserved? *Nat Immunol* 6: 973–979
- Bi G, Zhou Z, Wang W, Li L, Rao S, Wu Y, Zhang X, Menke FLH, Chen S, Zhou JM (2018) Receptor-like cytoplasmic kinases directly link diverse pattern recognition receptors to the activation of mitogen-activated protein kinase cascades in *Arabidopsis*. *Plant Cell* 30: 1543–1561
- Cao Y, Liang Y, Tanaka K, Nguyen CT, Jedrzejczak RP, Joachimiak A, Stacey G (2014) The kinase LYK5 is a major chitin receptor in *Arabidopsis* and forms a chitin-induced complex with related kinase CERK1. *Elife* 3: e03766–e03785
- Chen D, Cao Y, Li H, Kim D, Ahsan N, Thelen J, Stacey G (2017) Extracellular ATP elicits DORN1-mediated RBOHD phosphorylation to regulate stomatal aperture. *Nat Commun* 8: 2265–2278
- Clough SJ, Bent AF (1998) Floral dip: a simplified method for *Agrobacterium*-mediated transformation of *Arabidopsis thaliana*. *Plant J* 16: 735–743

- Couto D, Zipfel C (2016) Regulation of pattern recognition receptor signalling in plants. *Nat Rev Immunol* 16: 537–552
- Dow M, Newman MA, von Roepenack E (2000) The induction and modulation of plant defense responses by bacterial lipopolysaccharides. *Annu Rev Phytopathol* 38: 241–261
- Erbs G, Newman MA (2012) The role of lipopolysaccharide and peptidoglycan, two glycosylated bacterial microbe-associated molecular patterns (MAMPs), in plant innate immunity. *Mol Plant Pathol* 13: 95–104
- Gimenez-Ibanez S, Hann DR, Ntoukakis V, Petutschnig E, Lipka V, Rathjen JP (2009) AvrPtoB targets the LysM receptor kinase CERK1 to promote bacterial virulence on plants. *Curr Biol* 19: 423–429
- Gomez-Gomez L, Boller T (2000) FLS2: an LRR receptor-like kinase involved in the perception of the bacterial elicitor flagellin in *Arabidopsis*. *Mol Cell* 5: 1003–1011
- Jones JDC, Dangl JL (2006) The plant immune system. *Nature* 444: 323–329
- Kadota Y, Sklenar J, Derbyshire P, Stransfeld L, Asai S, Ntoukakis V, Jones JD, Shirasu K, Menke F, Jones A et al (2014) Direct regulation of the NADPH oxidase RBOHD by the PRR-associated kinase BIK1 during plant immunity. *Mol Cell* 54: 43–55
- Kagan JC (2017) Lipopolysaccharide detection across the kingdoms of life. *Trends Immunol* 38: 696–704
- Kim MG, da Cunha L, McFall AJ, Belkhadir Y, DebRoy S, Dangl JL, Mackey D (2005) Two *Pseudomonas syringae* type III effectors inhibit RIN4-regulated basal defense in *Arabidopsis*. *Cell* 121: 749–759
- Kutschera A, Dawid C, Gisch N, Schmid C, Raasch L, Gerster T, Schaffer M, Smakowska-Luzan E, Belkhadir Y, Vlot AC et al (2019) Bacterial medium-chain 3-hydroxy fatty acid metabolites trigger immunity in *Arabidopsis* plants. *Science* 364: 178–181
- Lal NK, Nagalakshmi U, Hurlburt NK, Flores R, Bak A, Sone P, Ma X, Song G, Walley J, Shan L et al (2018) The receptor-like cytoplasmic kinase BIK1 localizes to the nucleus and regulates defense hormone expression during plant innate immunity. *Cell Host Microbe* 23: 485–497
- Li L, Li M, Yu L, Zhou Z, Liang X, Liu Z, Cai G, Gao L, Zhang X, Wang Y et al (2014) The FLS2-associated kinase BIK1 directly phosphorylates the NADPH oxidase RbohD to control plant immunity. *Cell Host Microbe* 15: 329–338
- Lin W, Li B, Lu D, Chen S, Zhu N, He P, Shan L (2014) Tyrosine phosphorylation of protein kinase complex BAK1/BIK1 mediates *Arabidopsis* innate immunity. *Proc Natl Acad Sci USA* 111: 3632–3637
- Liu J, Elmore JM, Lin ZJ, Coaker G (2011) A receptor-like cytoplasmic kinase phosphorylates the host target RIN4, leading to the activation of a plant innate immune receptor. *Cell Host Microbe* 9: 137–146
- Liu J, Liu B, Chen S, Gong BQ, Chen L, Zhou Q, Xiong F, Wang M, Feng D, Li JF et al (2018) A tyrosine phosphorylation cycle regulates fungal activation of a plant receptor ser/thr kinase. *Cell Host Microbe* 23: 241–253
- Lu D, Wu S, Gao X, Zhang Y, Shan L, He P (2010) A receptor-like cytoplasmic kinase, BIK1, associates with a flagellin receptor complex to initiate plant innate immunity. *Proc Natl Acad Sci USA* 107: 496–501
- Luo X, Xu N, Huang J, Gao F, Zou H, Boudsocq M, Coaker G, Liu J (2017) A lectin receptor-like kinase mediates pattern-triggered salicylic acid signaling. *Plant Physiol* 174: 2501–2514
- Macho AP, Schwessinger B, Ntoukakis V, Brutus A, Segonzac C, Roy S, Kadota Y, Oh MH, Sklenar J, Derbyshire P et al (2014) A bacterial tyrosine phosphatase inhibits plant pattern recognition receptor activation. *Science* 343: 1509–1512
- Miya A, Albert P, Shinya T, Desaki Y, Ichimura K, Shirasu K, Narusaka Y, Kawakami N, Kaku H, Shibuya N (2007) CERK1, a LysM receptor kinase, is essential for chitin elicitor signaling in *Arabidopsis*. *Proc Natl Acad Sci USA* 104: 19613–19618
- de Oliveira MV, Xu G, Li B, de Souza Vespoli L, Meng X, Chen X, Yu X, de Souza SA, Intorne AC, de A Manhães AM et al (2016) Specific control of *Arabidopsis* BAK1/SERK4-regulated cell death by protein glycosylation. *Nat Plants* 2: 15218
- Park BS, Song DH, Kim HM, Choi BS, Lee H, Lee JO (2009) The structural basis of lipopolysaccharide recognition by the TLR4-MD-2 complex. *Nature* 458: 1191–1195
- Peng Y, Chen L, Li S, Zhang Y, Xu R, Liu Z, Liu W, Kong J, Huang X, Wang Y et al (2018) BRI1 and BAK1 interact with G proteins and regulate sugar-responsive growth and development in *Arabidopsis*. *Nat Commun* 9: 1522
- Perraki A, DeFalco TA, Derbyshire P, Avila J, Sere D, Sklenar J, Qi X, Stransfeld L, Schwessinger B, Kadota Y et al (2018) Phosphocode-dependent functional dichotomy of a common co-receptor in plant signalling. *Nature* 561: 248–252
- Poltorak A, He X, Smirnova I, Liu MY, Van Huffel C, Du X, Birdwell D, Alejos E, Silva M, Galanos C et al (1998) Defective LPS signaling in C3H/HeJ and C57BL/10ScCr mice: mutations in Tlr4 gene. *Science* 282: 2085–2088
- Ranf S, Gisch N, Schaffer M, Illig T, Westphal L, Knirel YA, Sanchez-Carballo PM, Zahringer U, Huckelhoven R, Lee J et al (2015) A lectin S-domain receptor kinase mediates lipopolysaccharide sensing in *Arabidopsis thaliana*. *Nat Immunol* 16: 426–433
- Ranf S (2016) Immune sensing of lipopolysaccharide in plants and animals: same but different. *PLoS Pathog* 12: e1005596–e1005603
- Rao S, Zhou Z, Miao P, Bi G, Hu M, Wu Y, Feng F, Zhang X, Zhou JM (2018) Roles of receptor-like cytoplasmic kinase VII members in pattern-triggered immune signaling. *Plant Physiol* 177: 1679–1690
- Rapicavoli JN, Blanco-Ulate B, Muszynski A, Figueroa-Balderas R, Morales-Cruz A, Azadi P, Dobruchowska JM, Castro C, Cantu D, Roper MC (2018) Lipopolysaccharide O-antigen delays plant innate immune recognition of *Xylella fastidiosa*. *Nat Commun* 9: 390–420
- Shi J, Zhao Y, Wang Y, Gao W, Ding J, Li P, Hu L, Shao F (2014) Inflammatory caspases are innate immune receptors for intracellular LPS. *Nature* 514: 187–192
- Shimazu R, Akashi S, Ogata H, Nagai Y, Fukudome K, Miyake K, Kimoto M (1999) MD-2, a molecule that confers lipopolysaccharide responsiveness on Toll-like receptor 4. *J Exp Med* 189: 1777–1782
- Silipo A, Erbs G, Shinya T, Dow JM, Parrilli M, Lanzetta R, Shibuya N, Newman MA, Molinaro A (2010) Glyco-conjugates as elicitors or suppressors of plant innate immunity. *Glycobiology* 20: 406–419
- Tang D, Wang G, Zhou JM (2017) Receptor kinases in plant-pathogen interactions: more than pattern recognition. *Plant Cell* 29: 618–637
- Tsuda K, Mine A, Bethke G, Igarashi D, Botanga CJ, Tsuda Y, Glazebrook J, Sato M, Katagiri F (2013) Dual regulation of gene expression mediated by extended MAPK activation and salicylic acid contributes to robust innate immunity in *Arabidopsis thaliana*. *PLoS Genet* 9: e1004015–e1004029
- Underwood W, Zhang S, He SY (2007) The *Pseudomonas syringae* type III effector tyrosine phosphatase HopAO1 suppresses innate immunity in *Arabidopsis thaliana*. *Plant J* 52: 658–672
- Wan J, Zhang XC, Neece D, Ramonell KM, Clough S, Kim SY, Stacey MG, Stacey G (2008) A LysM receptor-like kinase plays a critical role in chitin signaling and fungal resistance in *Arabidopsis*. *Plant Cell* 20: 471–481
- Xu N, Luo X, Li W, Wang Z, Liu J (2017) The bacterial effector AvrB-induced RIN4 hyperphosphorylation is mediated by a receptor-like cytoplasmic kinase complex in *Arabidopsis*. *Mol Plant Microbe Interact* 30: 502–512

- Yamada K, Yamashita-Yamada M, Hirase T, Fujiwara T, Tsuda K, Hiruma K, Saijo Y (2016) Danger peptide receptor signaling in plants ensures basal immunity upon pathogen-induced depletion of BAK1. *EMBO J* 35: 46–61
- Zhou J, Wang P, Claus LAN, Savatin DV, Xu G, Wu S, Meng X, Russinova E, He P, Shan L (2019) Proteolytic processing of SERK3/BAK1 regulates plant immunity, development, and cell death. *Plant Physiol* 180: 543–558
- Zipfel C, Robatzek S, Navarro L, Oakeley EJ, Jones JD, Felix G, Boller T (2004) Bacterial disease resistance in *Arabidopsis* through flagellin perception. *Nature* 428: 764–767
- Zipfel C, Kunze G, Chinchilla D, Caniard A, Jones JD, Boller T, Felix G (2006) Perception of the bacterial PAMP EF-Tu by the receptor EFR restricts *Agrobacterium*-mediated transformation. *Cell* 125: 749–760
- Zipfel C, Oldroyd GE (2017) Plant signalling in symbiosis and immunity. *Nature* 543: 328–336